Article

One Step Closer to an Ideal Insensitive Energetic Molecule: 3,5-Diamino-6-hydroxy-2-oxide-4-nitropyrimidone and its Derivatives

Jichuan Zhang, Yongan Feng, Yiyang Bo, Richard J. Staples, Jiaheng Zhang,* and Jean'ne M. Shreeve*

ACCESS | 📊 Metrics & More | 📖 Article Recommendations | 🔵SI Supporting Information

ABSTRACT: Reaching the goal of developing an insensitive high-energy molecule (**IHEM**) is a major challenge. In this study, 3,5-diamino-6-hydroxy-2-oxide-4-nitropyrimidone (**IHEM-1**) was synthesized in one step from 2,4,6-triamino-5-nitropyrimidine-1,3-dioxide hydrate (ICM-102 hydrate). The density of compound **IHEM-1** is 1.95 g cm^{-3} with a decomposition temperature of 271 °C. Its detonation velocity and pressure are 8660 m s^{-1} and 33.64 GPa, respectively, which are far superior to the detonation performance of 1,3,5-triamino-2,4,6-trinitrobenzene (TATB), while its sensitivity is identical with that of TATB. In addition, four derivatives (**1a**, chloride; **1b**, nitrate; **1c**, perchlorate; and **1d**, dinitramide) were prepared on the basis of the weak base site (N−O group) and show excellent energetic properties. By combining a series of advantages, including simple preparation, high yield, high density, very low solubility in aqueous solution, high thermostability, insensitivity, and excellent detonation performance, **IHEM-1** approaches an ideal insensitive high-energy molecule. Compounds **1b−1d** are also competitive as new high-energy-density materials.
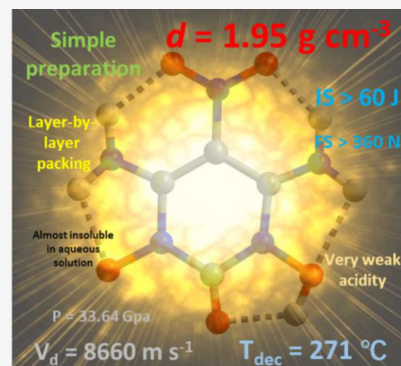
INTRODUCTION

Energetic compounds have played an essential role in defense and civilian industries since the time of Alfred Nobel.[1,2] Many compounds with excellent detonation performance have been explored for more than a hundred years.[3] However, owing to the competing properties of high energy and high safety,[4] accidents have occurred occasionally during the preparation, transportation, and application of high-energy-density materials because of their high sensitivities.[5] The development of insensitive high-energy molecules (IHEM) has become extremely important.[6] In particular, in the fields of nuclear weapons and space exploration, insensitive high-energy compounds are essential due to the special applied environments.[7] However, their evolution is slow. To date, the most commonly utilized insensitive energetic molecule is 2,4,6-triamino-1,3,5-trinitrobenzene (TATB), which was invented in 1888. Its detonation energy is only 65% of that of cyclotetramethylenetetranitramine (HMX), and therefore, it does not meet the requirements of a modern day insensitive energetic compound.[8−10]

New IHEMs, such as 2,4,6-triamino-3,5-dinitropyridine-1-oxide (TADNPyO),[11,12] the 3,9-diamino-4,8-dinitro-pyrazolo-triazine (DADNPT),[13] 2,4,6-triamino-5-nitropyrimidine-1,3-dioxide (ICM-102),[7] 3-nitro-1,2,4-triazol-5-one (NTO),[14] etc., have been explored over the past decades.[15] However, their further applications have been hindered for different reasons. TADNPyO has an oxygen balance similar to TATB (−55.6% vs −55.8%) but a lower density at room temperature than TATB (1.876 g cm^{-3} vs 1.937 g cm^{-3}). Density is directly propotional to detonation velocity, and the detonation

pressure increases with the square of the density. The preparations of TADNPyO and DADNP both involve tedious steps and even harsh reaction conditions, which increase the cost. The removal of H$_2$O from ICM-102 crystals involves temperatures as high as 178 °C or large quantities of organic solvents at 130 °C. This process often causes the collapse of crystals, which interferes with highly dense packing, and gives rise to a low-energy density. NTO is strongly acidic (pK_a = 3.67), which results in good solubility in aqueous solutions (160 g L^{-1}) and can corrode metallic equipment during long-term storage.[16] Therefore, in conclusion, an ideal insensitive high-energy molecule (IHEM) with promising applications should have not only a high density but also some notable drawbacks, such as complicated synthetic steps, strong acidity of resulting compounds, and the invariable presence of hydrates must be absent. Clearly, this is a huge challenge for molecular design and organic synthesis.

Planar molecular configurations accompanying layer-by-layer compact stacking (planar layered and wavelike layered, Scheme 1a) are less sensitive than other stacking modes because they can transform the mechanical energy acting on bulk material into relative motion between layers when they are subjected to

Scheme 1. (a) Variation Trend of Sensitivities for Compounds with Different Packings, (b) Variation of Densities in Several Compounds upon the Introduction of the Carbonyl Group, and (c) Title Compound in This Work
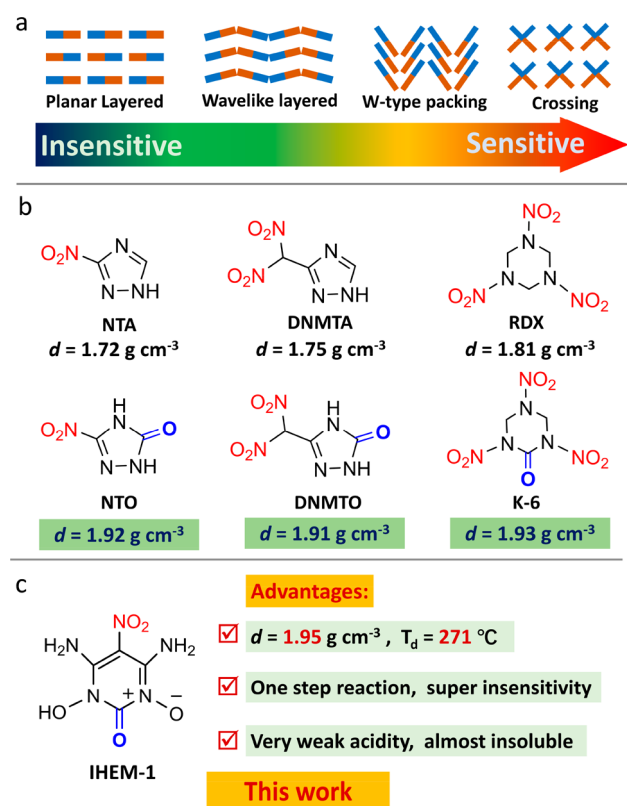
intense mechanical stimuli.[17−21] Additionally, the strong intermolecular hydrogen bonds formed with neighboring molecules and the close $\pi-\pi$ packing not only enhance the density of the resulting compound but also cause this kind of compound to be nearly insoluble in water, which decreases acidity and avoids hydrate formation. Examples of these species are TATB, 2,6-diamino-3,5-dinitropyridine-1-oxide (ANPyO), 1,1-diamino-2,2-dinitroethene (FOX-7), and TADNPyO.[8,15] Generally speaking, NO_2, N—O, and $NHNO_2$ are the traditional groups that result in high density in the resulting compounds;[22−24] unfortunately, these groups increase the sensitivity of the resulting compounds concomitantly. However, the carbonyl group also increases density significantly without a concomitant increase in sensitivity of the resulting compounds.[25,26] For example, the introduction of the C=O group into 3-nitro-1,2,4-triazole (NT),[27] 3-dinitromethanide-1,2,4-triazole (DNMT),[28] and cyclotrimethylenetrinitramine (RDX)[29] results in marked increases in density of the resulting compounds NTO, DNMTO, and K-6,[6,30,31] from 1.72, 1.75, and 1.81 to 1.92, 1.91, and 1.93 g cm^{-3}, respectively (Scheme 1b). The impact sensitivities (IS) are >60, 22, and 7.5 J, respectively, which are equal to or even less sensitive than their precursors. Surprisingly, the C=O group has not received much attention, although the insertion of a C=O group is more easily realized than more energetic groups.[32,33]

In view of the above, a new insensitive high-energy molecule, 3,5-diamino-6-hydroxy-2-oxide-4-nitropyrimidone (IHEM-1, Scheme 1c), which is planar and has layer-by-layer close stacking and a carbonyl group, was synthesized by a simple

reaction between 2,4,6-triamino-5-nitropyrimidine-1,3-dioxide monohydrate and dilute HNO_3 (1 M). **IHEM-1** is only very slightly soluble in water and has an experimental density of 1.95 g cm^{-3} at ambient temperature. Since its safety and synthetic feasibility are comparable to those of TATB, while displaying a higher energy density, **IHEM-1** is a potential substitute for TATB. Four energetic salts (**1a**, chloride; **1b**, nitrate; **1c**, perchlorate; and **1d**, dinitramide) with excellent energetic properties were also obtained with compound **IHEM-1** as the precursor.
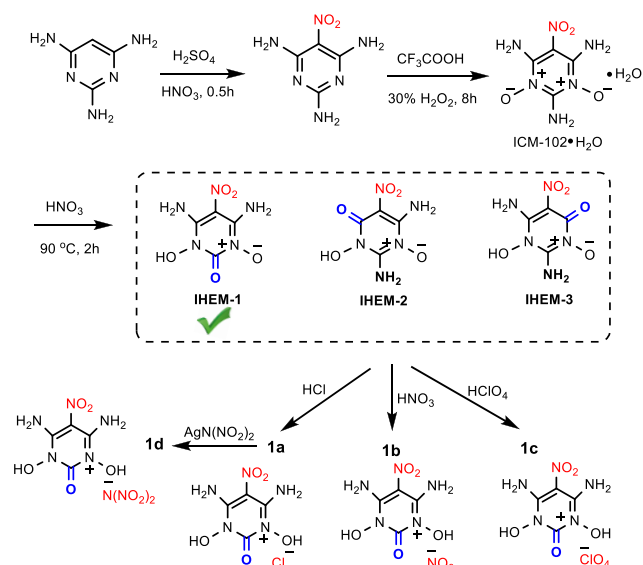
■ RESULTS AND DISCUSSION

Synthesis and Single-Crystal Structure. 2,4,6-Triamino-5-nitropyrimidine-1,3-dioxide monohydrate (ICM-102 hydrate) was synthesized simply in two steps in high yield from the commercial starting material, 2,4,6-triamino-pyrimidine.[7] ICM-102 nitrate was prepared by reaction of ICM-102 hydrate with 60% HNO_3 at room temperature.[34] However, when dilute HNO_3 (1 M) was utilized at 90 °C, a yellow precipitate (Figure S1) was formed after 2 h. The mixture was cooled to room temperature and the yellow precipitate was filtered and dried. Since the yellow precipitate is nearly insoluble in such solvents as H_2O, DMSO, and other organic solvents, ^1H and ^{13}C NMR spectra were not obtained, and a suitably sized crystal was not available for X-ray single-crystal diffraction. This made the confirmation of the molecular structure for the yellow precipitate difficult. However, its gas chromatography−mass spectrometry (GC−MS) spectrum shows that there is a main peak at 202 (Figure S2), and compared to its precursor in the infrared spectrum, it has a very strong characteristic peak assigned to C=O at 1738 (Figure S3). These two clues combined with the element analysis (Figure S4) show that the molecular formula is $C_4H_5N_5O_5$, and its molecular structure is most likely one selected from IHEM-1 to IHEM-3 (Scheme 1).

These three possible structures contain an N—O group, and NBO analysis shows that the charge values of the O atom (belonging to the N—O group) from **IHEM-1** to **IHEM-3** are −0.605, −0.660, and −0.578, respectively (Figures S5−S8), which are close to that of its precursor (ICM-102, − 0.651), thus the N—O sites in these three structures are the weak base sites. Here, in order to confirm its molecular structure, hydrochloric, nitric, and perchloric acids were used to react with the yellow precipitate, and compounds **1a**, **1b**, and **1c** (Scheme 2) were obtained directly from reactions between **IHEM-1** and the strong acids, respectively. The single-crystal structures (Figure 1) of **1a** and **1b** were obtained through slow evaporation from the corresponding reaction solutions, respectively. Clearly, from the crystal structures of **1a** and **1b**, the molecular structure of yellow precipitate was confirmed to be **IHEM-1**. In addition, compound **1d** was formed from a metathesis reaction between compound **1a** and silver dinitramide in dimethyl sulfoxide (DMSO). However, the neutral multinitro N-heterocyclic compounds, such as 3,4,5-trinitro-1H-pyrazole, 4-amino-3,5-dinitro-1H-pyrazole, or their silver salts, do not give the corresponding salts through reactions with **IHEM-1** (or **1a**). This is the case because these N-heterocyclic compounds are weaker acids than hydrochloric, nitric, and perchloric acids and neutral dinitramide.[35]

Compound **1a** crystallized (colorless plates) from a concentrated HCl solution in the orthorhombic (*Pbca*) group with a calculated density of 1.919 g cm^{-3} at 173 K. Each unit cell contains one 3,5-diamino-6-hydroxy-4-nitro-

Scheme 2. Synthesis of IHEM-1: 1a−1d

eight cations and eight nitrate anions. Just as the cation in compound **1a**, the cation is nearly planar, and the lengths of the four additional intramolecular H bonds are 2.193, 2.005, 1.971, and 2.156 Å. Each cation is surrounded by four nitrate anions and four cations through 11 H bonds (with lengths from 1.654 to 2.588 Å, Figure 1c and Figure S10), and each nitrate anion is surrounded by three cations through five H bonds. The H bond (1.654 Å) between NO_3 and OH is one of the shortest H bonds found in energetic compounds,[31,36] since IHEM-1 is less basic than ICM-102 (the length of the H bond in the same position in ICM-102 nitrate is 1.772 Å). Finally, the structure is connected by these intermolecular H bonds to form a face-to-face double-layered 2D network structure (Figure 1d).

A suitably sized crystal of **IHEM-1** was not available for X-ray single-crystal diffraction, even though its aqueous solution was cooled. Nevertheless, its powder X-ray diffraction (PXRD, Figure S11) and its images obtained via scanning electron microscopy (SEM, Figure S12) show it has good crystallinity.

The crystal structure of IHEM-1 was resolved in an ab initio manner from powder diffraction data. To solve this problem, we used a $C_4H_5N_5O_5$ molecular formula as an independent motif in a simulated annealing approach. An initial structure was obtained, then corrected by density functional theory (DFT) geometry optimization, and finally refined via the Rietveld method.[37,38] As shown in Figure 2a, the final structure obtained after refinement produced a good fit to the diffraction pattern, with R_p = 9.77% and R_{wp} = 13.82%. The compound crystallizes in a centrosymmetric orthorhombic system (space group *Pcab*), with lattice constants of a = 14.6278(9) Å, b = 13.8636(11) Å, c = 6.8291(3) Å, and V = 1384.90(15) Å^3. Its calculated density is an astonishing 1.949 g cm^{-3} at room temperature (Table S1). Similar to its precursor (ICM-102), it is a planar molecule, with five intramolecular hydrogen bonds

pyrimidone-2-oxide cation and one chloride anion, and each cation is surrounded by four chloride anions and four additional 3,5-diamino-6-hydroxy-4-nitropyrimidone-2-oxide cations through 6 H bonds (bond lengths between 2.158 and 2.423 Å, Figure 1a). The cation is nearly planar (except for the H atoms; Figure S9), and the four intramolecular hydrogen bonds have bond lengths of 2.151, 2.025, 2.036, and 2.146 Å. The crystal is connected by six intermolecular H bonds, forming a 2D wave-like network (Figure 1b).

Compound **1b** crystallized (colorless plate-needles) in the orthorhombic (*Pbca*) group with a calculated density of 1.959 g cm^{-3} at 173 K from a 70% HNO_3 solution. Each unit cell has
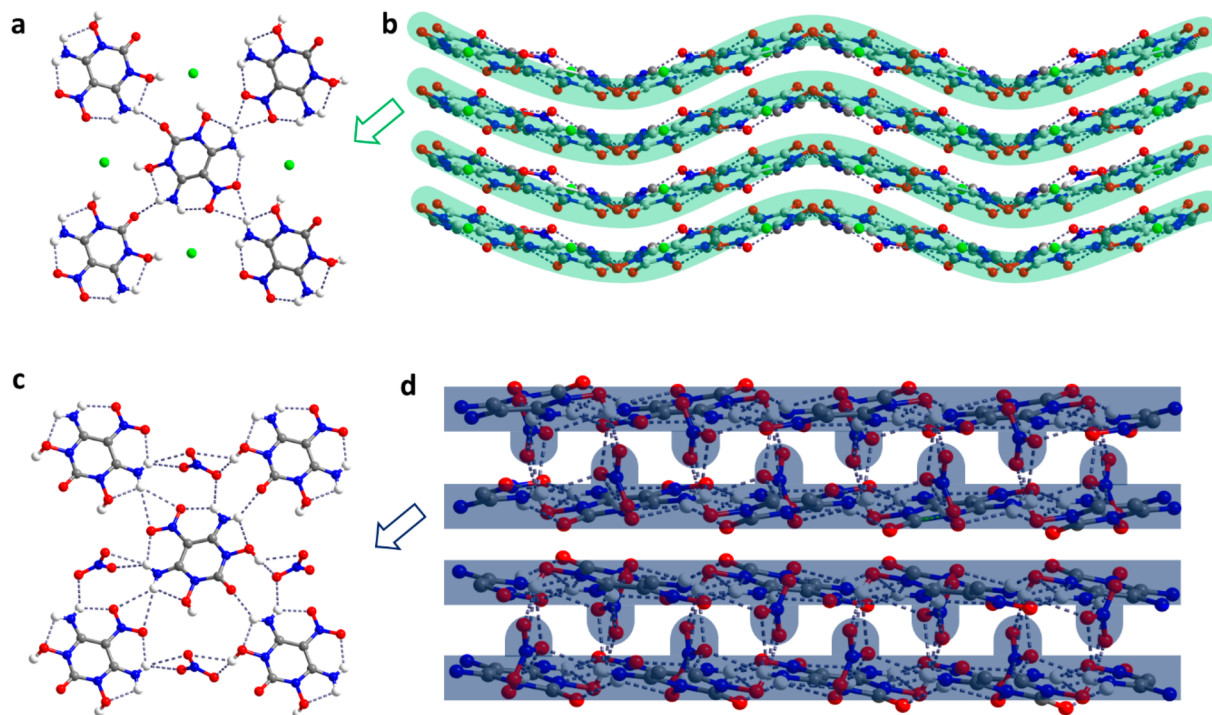

Figure 1. (a and b) Arrangement and packing mode of compound **1a**. (c and d) Arrangement and packing mode of **1b** (atom color: C, black gray; H, gray; N, blue; O, red; Cl, green; H-bonds, blue-gray dashed line).
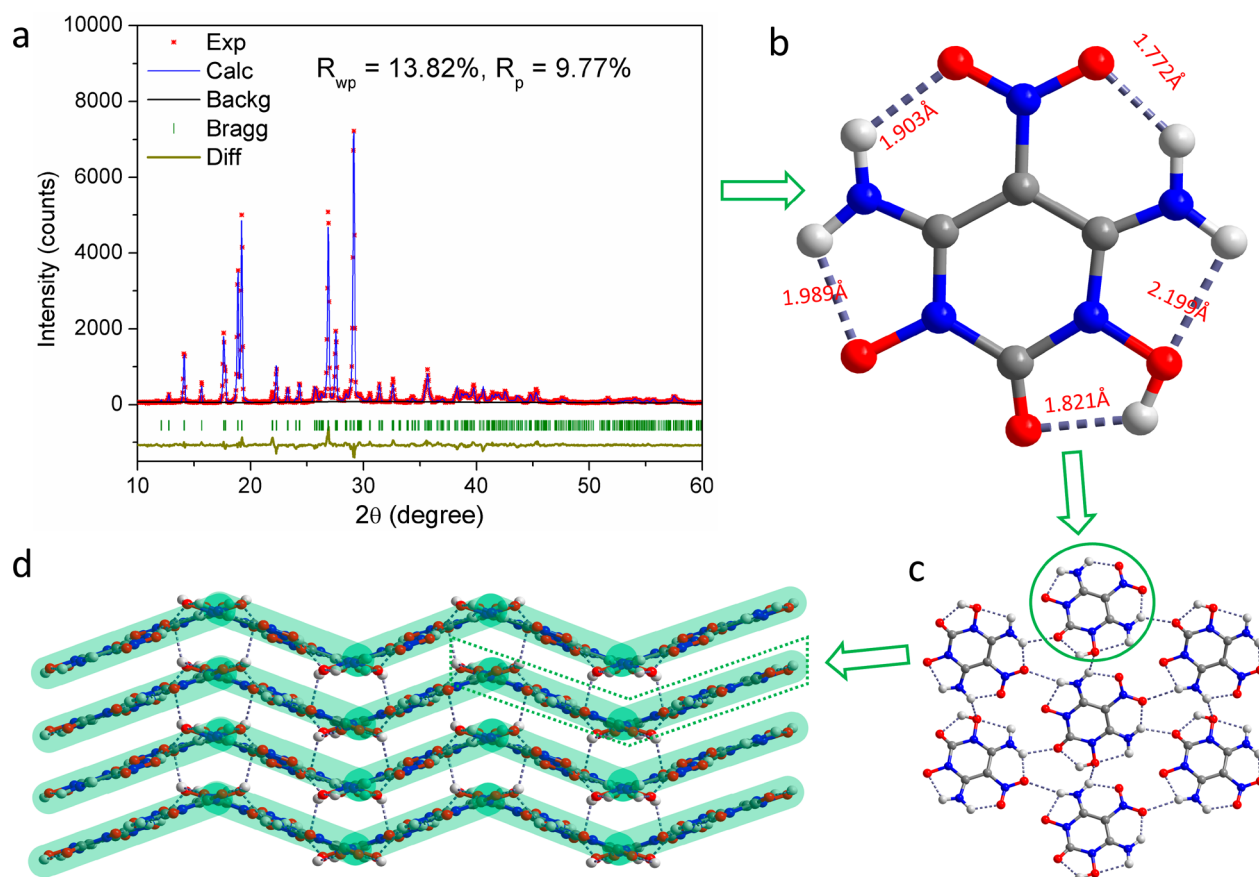
Figure 2. (a) PXRD (powder X-ray diffraction) pattern and Rietveld refinement of **IHEM-1** structure. (b) Single-molecular structure. (c) Single-layer arrangement of IHEM-1. (d) Layer-by layer packing of IHEM-1 (atom color: C, black gray; H, gray; N, blue; O, red; H bonds are blue-gray dashed lines).

with lengths of 1.772, 1.821, 1.903, 1.989, and 2.199 Å (Figure 2b). Compound **IHEM-1** has a wavelike two-dimensional layer-by-layer stacking with a distance of 3.15 Å (Figure S13), and in each layer, each molecule is bonded with six surrounding molecules through six intermolecular H bonds (Figure 2c, three coupled H bonds at 2.114, 2.263, and 2.485 Å). The two-dimensional layers are connected by intermolecular hydrogen bonds, thus forming a 3D network (Figure 2d).

It was worthwhile to investigate the mechanism of the formation of **IHEM-1**. Since ICM-102 is a weak base, it forms salts with strong acids (HNO_3, $HClO_4$, etc.) and it forms a cocrystal with HIO_3, a moderately strong acid.[34,36] Given that ICM-102 forms a monocation with an excess of strong acids, on the basis of the literature,[32,33,39,40] the reaction mechanism is believed to be the hydrolysis reaction catalyzed by HNO_3, and the supposed reaction steps may be as shown in Scheme 2a. When ICM-102 interacts with a strong acid, the basic site (O atom of the N−O group) is protonated to form a cation (step 1) (Scheme 3). Under the conditions of excess acid and a high temperature, the proton is transferred from the ring to the NH_2 moiety, forming an NH_3^+ group (step 2). Subsequently, in the presence of H_2O, the intermediate species formed in step 2 is changed to the unstable species in step 3. Then, NH_3 is lost to give **IHEM**-1. Believing this mechanism, other strong acids ($HClO_4$, H_2SO_4, HCl) were tried, and **IHEM-1** was invariably obtained in similar yields (68%−75%). Iodic, oxalic, and acetic acids also reacted with ICM-102 to give **IHEM-1** at ~90 °C.

Scheme 3. Proposed Reaction Mechanism of IHEM-1
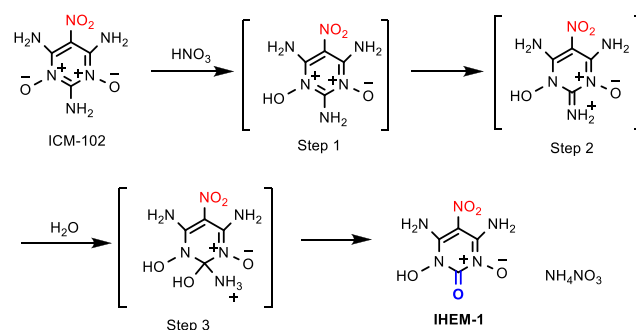
Thermostability and Sensitivity. The thermostabilities of **IHEM-1** and **1a−1d** were determined by using differential scanning calorimetry (DSC) at 5 °C min^{-1} in a nitrogen atmosphere, and the onset decomposition temperatures of these five compounds are 271, 270, 175, 142, and 152 °C (Table 1, Figures S14−S19), respectively. Among them, the decomposition temperature of **IHEM-1** is not only higher than that of the precursor, ICM-102,[7] but also notably higher than those of the carbonyl-containing compounds vide supra[6,15,25,26,30] and is comparable to that of HMX,[19] Since **IHEM-1** exhibits excellent thermal stability, Kissinger and Ozawa[29] methods were employed to investigate its thermodynamic properties and compare them with those of traditional heat-resistant energetic compounds. The differential scanning

Table 1. Physical Properties of IHEM-1 and its Derivatives, TATB, NTO, RDX, and HMX

compound	$T_d{}^a$ (°C)	ρ^b (g cm^{-3})	$\Delta_f H^{oc}$ (kJ mol^{-1})	$D_v{}^d$ (m s^{-1})	P^e (GPa)	IS^f (J)	FS^g (N)	OB^h (%)
IHEM-1	271	1.95	−204.5	8660	33.64	>60	>360	−43.35
1a	270	1.88	−262.9	7774	25.52	>60	>360	−40.07
1b	175	1.92	−343.1	8698	35.72	10	240	−18.03
1c	142	2.01	−302.0	8841	36.98	6	160	−10.54
1d	152	1.93	+139.4	9337	40.51	7	240	−10.32
TATB^i	315	1.94	−139.5	8114	32.4	>60	>360	−55.81
NTO^j	237	1.92		8446	32.90	>60	>360	−24.62
RDX^k	205	1.81	+80.0	8795	34.90	7.5	120	−21.61
HMX^k	270	1.91	+74.8	9144	39.20	7.5	120	−21.61

^{a}Decomposition temperature (onset). ^{b}Experimental density at room temperature. ^{c}Enthalpy of formation (kJ mol^{-1}). ^{d}Detonation velocity (m s^{-1}). ^{e}Detonation pressure (GPa). ^{f}Impact sensitivity (J). ^{g}Friction sensitivity (N). ^{h}Oxygen balance calculated using OB = (O-2C-1 − 2H)1600/ M}. ^{i}Refs 7 and 41. ^{j}Refs 42 and 43. ^{k}Refs 31, 44, and 45.

calorimetry (DSC) profile of IHEM-1 at different heating rates is shown in Figure 3. The apparent activation energies (E)
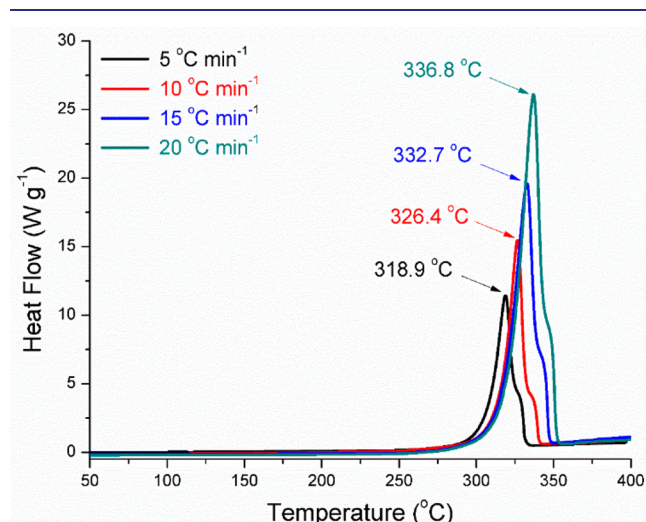

Figure 3. DSC curves of **IHEM-1** at different heating rates.

obtained by the two methods agree well with each other at 220.3 and 219.0 kJ mol^{-1}, respectively. The correlation coefficients (r^2) of these two methods are 0.9965 and 0.9968, respectively, very close to 1, which indicates that the results are reliable. The activation energies of **IHEM-1** obtained using these methods are higher than that of TATB (211 kJ mol^{-1}),[13] thus showing that **IHEM-1** has a better heat resistance than TATB. Excellent thermostability and heat resistance depend mainly on intramolecular factors, such as bond dissociation energies (BDEs)[46] and intramolecular hydrogen bonds.[47,48] The C−NO$_2$, and N−O bonds, which possibly lead to the initial decomposition of **IHEM-1**, have been investigated by BDE calculations, and the results show that the BDEs of C−NO$_2$ in **IHEM-1**, TATB, ICM-102, and NTO are 290.49, 290.46, 321.92, and 274.72 kJ mol^{-1}, respectively (Table 2), and the BDEs of N−O in **IHEM-1** and ICM-102 are 455.31 and 474.44 kJ mol^{-1}, respectively. The BDE of C−NO$_2$ in **IHEM-1** is higher than those in TATB and NTO, although the BDEs of C−NO$_2$ and N−O in **IHEM-1** are lower than those in ICM-102; the average intramolecular hydrogen bond length in **IHEM-1** is 1.937 Å (Table S6), which is shorter than that in ICM-102 (2.168 Å) but longer than that in TATB (1.810 Å). Because the intramolecular hydrogen bond is another factor to enhance the conjugation

Table 2. Molecular Simulations of IHEM-1 and Typical Insensitive Molecules

compound	IHEM-1	TATB	ICM-102	NTO
BDE of C−NO$_2$ (kJ mol^{-1})	290.49	290.46	321.92	274.72
BDE of N−O (kJ mol^{-1})	455.31		474.44	
bond order of C−NO$_2$	0.903	0.898	0.897	0.786
bond order of N−O	1.141		1.127	

effect in the molecule and to stabilize the system. Comprehensively, a high BDE and short intramolecular hydrogen bonds give rise to high thermostability and heat resistance for **IHEM-1**. Therefore, **IHEM-1** is an excellent candidate as a heat-resistant energetic molecule.

Sensitivities toward impact and friction, determined using BAM (Bundesanstalt für Materialforschung and -Prüfung) standards, show that **IHEM-1** has a very low sensitivity to impact and friction stimulation with values similar to those of TATB (impact sensitivity, IS > 60 J, and friction sensitivity, FS > 360 N).[7,15] Compound **1a** is also insensitive to impact and friction at higher than 60 J and 360 N, respectively. The impact and friction sensitivities of compounds **1b**−**1d** were determined to be 10, 6, and 7 J, and 240, 160, and 240 N, respectively. The extremely low sensitivity of **IHEM-1** is further explained from both molecular and crystal levels. At the molecular level, it is known that higher bond orders,[49,50] more negative ESP,[51] and an average deviation of ESP approaching 0.25[52] result in low sensitivity of an energetic molecule. Compared with those of TATB, ICM-102, and NTO, the bond orders of C−NO$_2$ and N−O in **IHEM-1** are 0.903 and 1.141, respectively (Table 2 and Tables S2−S5). The C−NO$_2$ bond order in **IHEM-1** is not only higher than that of its precursor (ICM-102, 0.897) but also higher than those in TATB (0.896, and NTO (0.786). The N−O bond order of **IHEM-1** is higher than that in ICM-102 (1.127). The most negative ESP in **IHEM-1** is −56.05, clearly lower than those in TATB, ICM-102, and NTO. Meanwhile, the average deviation of ESP in **IHEM-1** is 0.249 (Figure 4a, Table 2, and Figures S20−S23), which is very close to 0.25, and higher than those of three insensitive molecules. Additionally, from the view of crystal structure and compared to its precursor ICM-102 and to TATB, the planar **IHEM-1** molecule is trapped by intermolecular hydrogen bonds not only from the same layer but also from neighboring layers. The distance between layers is 3.15 Å (Figure S13), shorter than that in ICM-102 (3.19 Å, Table S6) and only slightly longer than that in TATB (3.14 Å), which shows that the $\pi-\pi$ interactions between layers in
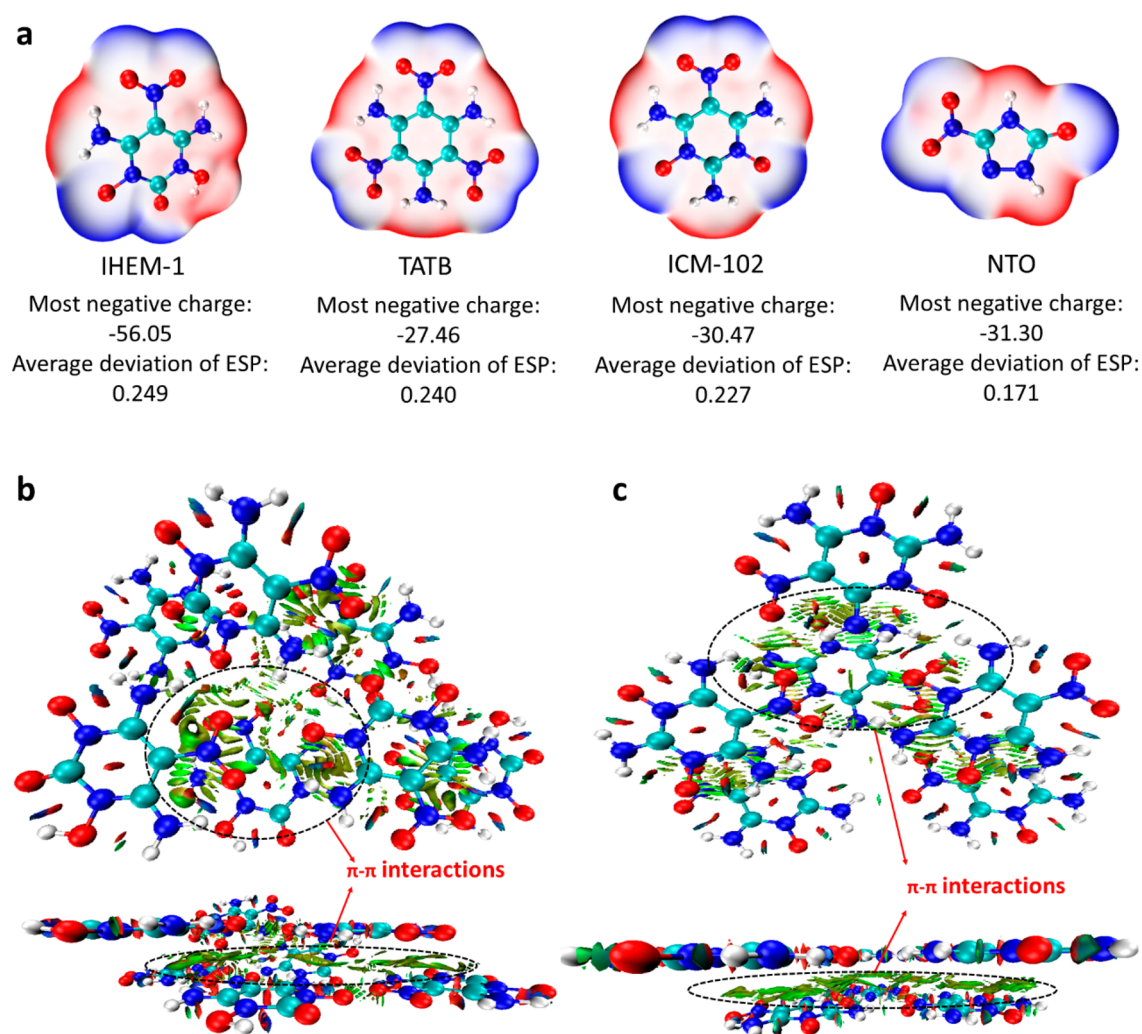
Figure 4. (a) Calculations of ESP for **IHEM-1**, TATB, ICM-102, and NTO. (b and c) Noncovalent interaction (NCI) plots of IHEM-1(b) and ICM-102 (c). The surfaces are colored on a blue−green−red scale indicating strong attractive interactions, weak attractive, and strong nonbonded overlap, respectively (upper, layer−layer viewpoint, down, layer−layer overlap viewpoint).

IHEM-1 are stronger than that of ICM-102. This is supported by NCI calculations (Figure 4b,c and Figure S24), where the green areas in **IHEM-1** are larger than that in ICM-102.[31,53] Notably, the close layer-by-layer stacking of **IHEM-1** could consume mechanical energy acting on the bulk material, leading to the formation of local hot spots.[9,54] A high BDE, short intramolecular hydrogen bonds, high bond orders, low negative ESP, and a close to 0.25 of the average deviation of ESP, layer−layer structure, strong $\pi-\pi$ interactions, and compact packing through multihydrogen bonds are positive factors that contribute markedly to the excellent thermal stability and insensitivity of IHEM-1 to heat, impact, and friction, respectively, which ensures its high potential as a new insensitive high-energy molecule.

Solubility, Acidity, and Density. The solubility of **IHEM-1** in water is limited and it is even lower in organic solvents, such as DMSO, MeOH, EtOH, acetonitrile (MeCN), dimethylformamide (DMF), and ethyl acetate (EA). Its solubility was determined to be 6.75 mg in 100 mL of water at room temperature (25 °C),[55] and even at 100 °C, its solubility is only 28.1 mg in 100 mL, which is significantly lower than those of ICM-102 and NTO (220 and 1600 mg in 100 mL of water at room temperature, respectively),[7,16] This

low solubility may arise from the abundance of short intermolecular H-bonds. The same is true for compound **1b**. The solubility of compound **1b** was found to be 23 mg in 100 mL of water at room temperature. The low solubilities of **IHEM-1** and **1b** support their further applications because problems caused by hygroscopicity and moisture are avoided. Additionally, the low solubility causes the molecules to be friendly to biological systems and the environment, since they will not poison or pollute through being dissolved in aqueous solutions.

NBO analysis gives a charge value of the H bonded to the N−OH group at 0.550, which suggests a strongly acidic behavior for **IHEM-1**. However, the pH of **IHEM-1** in a saturated solution was determined to be 5.33, which is similar to that of normal rain (5.0−5.5),[56] and its pK_a was determined to be 6.17,[57] thus it is a very weak acid. The pH of NTO in a saturated solution was determined to be 2.33, and its pK_a is 3.67, which is notably higher than that of IHEM-1. The weak acidity of **IHEM-1** is due to the poor solubility and the strong intramolecular H bonds (measuring 1.821 Å), which limit dissociation. Properties such as low solubility and very weak acidity do make **IHEM-1** noncorrosive to the metallic parts of equipment and devices.

The densities of **IHEM-1** and **1a−1d** were determined using a gas pycnometer to be 1.95, 1.87, 1.92, 2.01, and 1.93 g cm^{-3}, respectively. The density of **IHEM-1** is not only much higher than that of its precursor (anhydrous ICM-102, 1.85 g cm^{-3} at 298 K, Table S7) but also higher than those of TATB and NTO. The calculation of the packing index values shows that the packing index of **IHEM-1** is 79.1% at room temperature (Figure 5 and Table S8), which is not only higher than those of
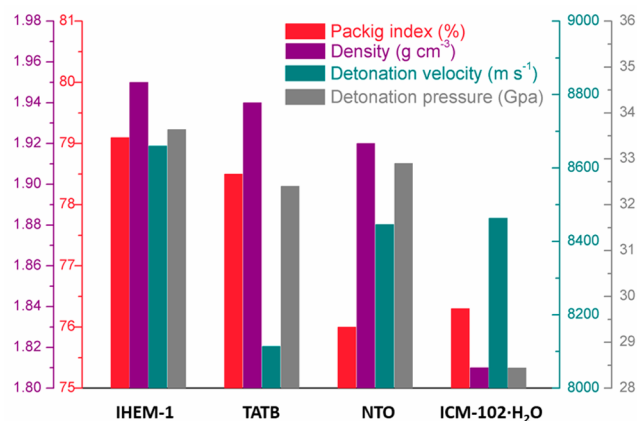

Figure 5. Packing indices, detonation performance, and densities of several energetic compounds.

TATB (78.5%) and NTO (76.0%) but also higher than the majority of 380 randomly collected energetic molecules at room temperature (Figure S25). Among these energetic molecules, only two compounds (dihydroxylammonium 5,50-bistetrazole-1,10-diolate[58] and 4,8-dihydrodifurazano[3,4-b,e]-pyrazine[59]) with packing indices of 79.6% and 79.3%, respectively, were higher. Although the packing index of compound **1b** (76.9%) is lower than that of ICM-102 nitrate (78.0%),[34] it has a better oxygen content, leading to a good density (1.922 g cm^{-3} at 298 K),[60] which is comparable to that of ICM-102 nitrate (1.919 g cm^{-3} at 298 K).

Detonation Properties. Detonation performance was evaluated by calculating the detonation velocity (D_v) and detonation pressure (P) using the experimental density and the calculated heat of formation. The heats of formation of **IHEM-1** and **1a−1d** were calculated, according to the literature,[31,34] to be −204.5, −262.9, −343.1, −302.0, and +139.4 kJ mol^{-1} (Table 1 and Tables S7 and S9), respectively. With experimental densities in hand, the detonation performance of **IHEM-1** and **1a−1d** was achieved using EXPLO 5 software (6.01 version).[61] As shown in Table 1, the detonation velocity and detonation pressure of **IHEM-1** are 8660 m s^{-1} and 33.64 GPa, respectively. Although the insertion of the carbonyl group leads to a lower heat of formation than that of its precursor, its higher oxygen balance and higher density result in the detonation performance for **IHEM-1**, which is superior to those of ICM-102, NTO, and TATB and comparable to that of RDX. Compounds **1b−1d** also exhibit excellent detonation performance. Their detonation velocities and pressures are calculated to be 7774, 8698, 8841, and 9337 m s^{-1} and 25.52, 35.72, 36.98, and 40.51 GPa, respectively. It is noteworthy that the detonation properties of **1d** are higher than those of HMX.

■ CONCLUSION

A new insensitive high-energy compound, 3,5-diamino-6-hydroxy-2-oxide-4-nitropyrimidone (**IHEM-1**), with high density, high thermal stability, extremely low mechanical sensitivity, and excellent detonation performance was synthesized easily through the acidic hydrolysis of 2,4,6-triamino-5-nitropyrimidine-1,3-dioxide (ICM-102). Its wavelike two-dimensional layer-by-layer stacking pattern was confirmed by employing PXRD analysis. Coupled with its other two advantages of low solubility and weak acidity, **IHEM-1** is very close to being an ideal, promising insensitive high-energy compound needed to replace TATB. Additionally, four derivatives with high densities and good detonation performance were also synthesized and are attractive as new high-energy-density materials.

■ EXPERIMENTAL SECTION

Safety Precautions. Although none of the energetic MOFs described herein exploded or detonated in the course of this research, these materials should be handled with extreme care using the best safety practices.

General Methods. All reagents were purchased from AKSci or Alfa Aesar in analytical grade and were used as supplied. ^{1}H NMR and ^{13}C NMR spectra were recorded on a 300 MHz (Bruker AVANCE 300) nuclear magnetic resonance spectrometer. Chemical shifts for ^{1}H NMR and ^{13}C NMR spectra are given with respect to $(CH_3)_4$Si (^{1}H and ^{13}C). DMSO-d_6 was used as a locking solvent unless otherwise stated. IR spectra were recorded using KBr pellets with a FT-IR spectrometer (Thermo Nicolet AVATAR 370). Density was determined at room temperature by employing a Micromeritics AccuPyc II 1340 gas pycnometer. Decomposition temperature (onset) was recorded using dry nitrogen gas at a heating rate of 5 °C min^{-1} and different rates (5, 10, 15, and 20 °C min^{-1}, respectively) on a differential scanning calorimeter (DSC, TA Instruments Q2000). Thermal behavior was also recorded by thermogravimetric analysis (TGA, TA Q50). Elemental analyses (C, H, N) were performed with a Vario Micro cube Elementar Analyzer. Impact and friction sensitivity measurements were carried out using a standard BAM Fallhammer and a BAM friction tester.

Computational Methods. The gas phase enthalpies of formation were calculated on the basis of the G2 method. The solid-state heat of formation of **IHEM-1** was calculated on the basis of Trouton's rule according to eq 1 (T represents either the melting point or the decomposition temperature when no melting occurs prior to decomposition).[62]

$$\Delta H_{sub} = 188 \, \text{J mol}^{-1} \text{K}^{-1} \times T \qquad (1)$$

For energetic salts (**1a−1d**), the solid-phase enthalpies of formation were obtained using a Born−Haber energy cycle.[63,64]

Crystal Structure Analysis. The molecular structure (**IHEM-1**) was deduced from the single-crystal structure of its nitrate salt (**1b**), and then, the pure **IHEM-1** was confirmed by its elemental analysis. When the pure **IHEM-1** was scanned by X-ray powder diffraction, the crystal structure of **IHEM-1** was resolved in an ab initio manner from powder diffraction data. The indexing of the diffraction pattern was readily realized using the DICVOL91 program.[65] The program suggested orthorhombic lattices for the title compound, with lattice constants of a = 14.6278(9) Å, b = 13.8636(11) Å, c = 6.8291(3) Å, and V = 1384.90(15) Å^3. The examination of diffraction extinctions reveals that the unit cells are primitive, and the extinction conditions corresponding to three glide planes of c, a, and b can be confirmed, suggesting that the space groups should be Pcab. To solve the crystal structure, we used $C_4H_5N_5O_5$ molecules as independent motifs in a simulated annealing approach. An initial structure is successfully obtained on the basis of the Powder Solve module implemented in software Reflex. Then, this initial crystal structure is corrected by density functional theory (DFT) geometry optimization and finally

refined via the Rietveld method.[37,38] As shown in Figure 2b, the final structure obtained after refinement produced a good fit to the diffraction pattern, with R_p = 9.77% and R_{wp} = 13.82%. The compound crystallizes in a centrosymmetric orthorhombic system (space group *Pcab*), with eight $C_4H_5N_5O_5$ molecules located in the general positions. The detailed crystallographic information is listed in Table S1.

A colorless plate-shaped crystal of **1a** with dimensions 0.25 × 0.13 × 0.07 mm³ was mounted on a nylon loop with Paratone oil. Data were collected using a Bruker APEX-II CCD diffractometer equipped with an Oxford Cryosystems low-temperature device, operating at T = 173(2) K. Data were measured using ε of −0.50° per frame for 100.83 s using Mo Kα radiation (sealed tube, 50 kV, 40 mA). The total number of runs and images was based on the strategy calculation from the program COSMO (BRUKER, V1.61, 2009). The achieved resolution was Θ = 26.025. A colorless plate-needle-shaped crystal of **1b** with dimensions 0.24 × 0.08 × 0.04 mm³ was mounted on a nylon loop with Paratone oil. Data were collected using a Bruker APEX-II CCD diffractometer equipped with an Oxford Cryosystems low-temperature device, operating at T = 173(2) K. Data were measured using ε of −0.50° per frame for 200.83 s using Mo Kα radiation (sealed tube, 50 kV, 40 mA). The total number of runs and images was based on the strategy calculation from the program COSMO (BRUKER, V1.61, 2009). The achieved resolution was Θ = 26.064.

Synthesis of Compound IHEM-1. Hydrated ICM-102 ($C_4H_6N_6O_4 \cdot H_2O$) was synthesized in two steps in high yield based on the literature.[7] The hydrated ICM-102 (0.44 g, 2 mmol) was added to water (60 mL), which was heated to 90 °C, and then, HNO$_3$ (3 mL, 1 mmol mL^{-1}, 1 M) was added to the mixture, which was stirred at this temperature for 2 h. A yellow precipitate formed, and the mixture was cooled to room temperature, filtered, and dried; 0.31 g (76.4% yield) of the resulting compound, **IHEM-1**, was obtained. IR (KBr): ν 3372, 3266, 1738, 1627, 1516, 1392, 1291, 1207, 1101, 949, 757, 634 cm^{-1}. $C_4H_5N_5O_5$ (203.11): calcd, C 23.65, H 2.48, N 34.48%; found, C 23.63, H 2.59, N 34.80%.

General Method for Preparing 1a−1c. Compound **IHEM-1** (0.406 g, 2 mmol) was added to concentrated HCl (15 mL), 70% HNO$_3$ (15 mL), or 70% HClO$_4$ (10 mL), respectively. After stirring for 30 min, the solution was filtered and put in a quiet place for slow evaporation (about 1−2 days). Crystal samples of **1a−1c** were collected and washed with a small amount of water (5 mL). Finally, **1a** (0.35g, 73% yield), **1b** (0.43 g, 81% yield), and **1c** (0.39 g, 64% yield) were obtained, as well as the crystals of **1a** and **1b** suitable for X-ray single-crystal diffraction analysis.

Compound 1a. Colorless crystal. ^{1}H NMR (DMSO-d_6): δ 9.83 (s, 4H). ^{13}C NMR (DMSO-d_6): δ 152.0, 143.3, 103.5 ppm. IR (KBr): ν 3369, 3238, 2915, 1767, 1634, 1526, 1412, 1298, 1203, 1104, 977, 703, 648 cm^{-1}. $C_4H_6ClN_5O_5$ (239.57): calcd, C 20.05, H 2.52, N 29.23%; found, C 19.76, H 2.57, N 29.20%.

Compound 1b. Colorless crystal. ^{1}H NMR (DMSO-d_6): δ 9.88 (s, 4H). ^{13}C NMR (DMSO-d_6): δ 152.0, 143.5, 103.6 ppm. IR (KBr): ν 3388, 3277, 1769, 1661, 1528, 1431, 1381, 1298, 1209, 1104, 1038, 975, 828, 765, 705, 628 cm^{-1}. $C_4H_6N_6O_8$ (266.13): calcd, C 18.05, H 2.27, N 31.58%; found, C 17.60, H 2.40, N 31.51%.

Compound 1c. Colorless crystal. ^{1}H NMR (DMSO-d_6): δ 9.86 (s, 4H). ^{13}C NMR (DMSO-d_6): δ 152.00, 143.5, 103.7 ppm. IR (KBr): ν 3373, 3261, 1776, 1757, 1655, 1526, 1380, 1305, 1248, 1221, 1199, 1102, 980, 768, 697, 626 cm^{-1}. $C_4H_6ClN_5O_9$ (303.57): calcd, C 15.83, H 1.99, N 23.07%; found, C 15.68, H 2.06, N 23.06%.

Synthesis of Compound 1d. Compound **1a** (0.24g, 1 mmol) was dissolved in DMSO (10 mL), and AgN(NO$_2$)$_2$ (0.22g, 1 mmol) was dissolved in DMSO (5 mL). After both were dissolved completely, the solutions were combined. The precipitate was filtered, and water (40 mL) was added to the filtrate. A white precipitate formed and was filtered and dried to give 0.19 g (62% yield) of **1d**. ^{1}H NMR (DMSO-d_6): δ 9.89 (s, 4H). ^{13}C NMR (DMSO-d_6): δ 152.0, 143.5, 103.7 ppm. IR (KBr): ν 3371, 3238, 2920, 1768, 1663, 1633, 1525, 1419, 1380, 1298, 1202, 1104, 1028, 977, 767, 702, 643 cm^{-1}. $C_4H_6N_8O_9$ (310.14): calcd, C 15.49, H 1.95, N 36.13%; found, C 15.91, H 2.19, N 35.22%.

■ ASSOCIATED CONTENT

Ⓢ Supporting Information

The Supporting Information is available free of charge at https://pubs.acs.org/doi/10.1021/jacs.1c05292.

Figures of yellow powder precipitate image, GC−MS spectrum, IR spectrum, elemental analysis, NBO distributions, single-crystal and packing modes, XRD pattern, SEM images, TGA curves, DSC curves, ESP calculations, NCI $\pi-\pi$ interactions, and statistics of packing index vs density, tables of crystallographic data and structure refinement parameters, bond orders, hydrogen bond lengths and layer distance, physical properties, packing index and densities, statistics of packing index vs density, and enthalpies of the species, and scheme of isodesmic reactions, (PDF)

Accession Codes

CCDC 2008342−2008343 and 2062676 contain the supplementary crystallographic data for this paper. These data can be obtained free of charge via www.ccdc.cam.ac.uk/data_request/cif, or by emailing data_request@ccdc.cam.ac.uk, or by contacting The Cambridge Crystallographic Data Centre, 12 Union Road, Cambridge CB2 1EZ, UK; fax: +44 1223 336033.

■ AUTHOR INFORMATION

Corresponding Authors

Jiaheng Zhang − *Sauvage Laboratory for Smart Materials, Harbin Institute of Technology, Shenzhen 518055, China;* ◉ orcid.org/0000-0002-2377-9796; Email: zhangjiaheng@hit.edu.cn

Jean'ne M. Shreeve − *Department of Chemistry, University of Idaho, Moscow, Idaho 83844-2343, United States;* ◉ orcid.org/0000-0001-8622-4897; Email: jshreeve@uidaho.edu

Authors

Jichuan Zhang − *Department of Chemistry, University of Idaho, Moscow, Idaho 83844-2343, United States; Shenzhen Institute of Advanced Technology, Chinese Academy of Sciences, Shenzhen 518055, China*

Yongan Feng − *School of Environmental and Safety Engineering, North University of China, Taiyuan 030051, China;* ◉ orcid.org/0000-0001-8456-5065

Yiyang Bo − *Sauvage Laboratory for Smart Materials, Harbin Institute of Technology, Shenzhen 518055, China*

Richard J. Staples − *Department of Chemistry, Michigan State University, East Lansing, Michigan 48824, United States;* ◉ orcid.org/0000-0003-2760-769X

Complete contact information is available at:
https://pubs.acs.org/10.1021/jacs.1c05292

Notes

The authors declare no competing financial interest.

■ REFERENCES

(1) Agrawal, J. P.; Hodgson, R. D. *Organic chemistry of explosives*; Wiley Online Library, 2007.

(2) Akhavan, J. *The chemistry of explosives*; Royal Society of Chemistry, 2011.

(3) Klapötke, T. M. Chemistry of high-energy materials; Walter de Gruyter GmbH & Co KG, 2019.

(4) Politzer, P.; Murray, J. S. High performance, low sensitivity: conflicting or compatible? *Propellants, Explos., Pyrotech.* 2016, 41, 414−425.

(5) Pichtel, J. Distribution and fate of military explosives and propellants in soil: a review. *Appl. Environ. Soil Sci.* 2012, 2012, 617236.

(6) Sikder, A.; Sikder, N. A review of advanced high performance, insensitive and thermally stable energetic materials emerging for military and space applications. *J. Hazard. Mater.* 2004, 112, 1−15.

(7) Wang, Y.; Liu, Y.; Song, S.; Yang, Z.; Qi, X.; Wang, K.; Liu, Y.; Zhang, Q.; Tian, Y. Accelerating the discovery of insensitive high-energy-density materials by a materials genome approach. *Nat. Commun.* 2018, 9, 2444.

(8) Rice, S. F.; Simpson, R. L. *The unusual stability of TATB (1, 3, 5-triamino-2, 4, 6-trinitrobenzene): A review of the scientific literature, technical Report*. U.S. Department of Energy, 1990.

(9) Zhang, C. Investigation of the slide of the single layer of the 1, 3, 5-triamino-2, 4, 6-trinitrobenzene crystal: sliding potential and orientation. *J. Phys. Chem. B* 2007, 111, 14295−14298.

(10) Dong, H. The development and countermeasure of high energy density materials. *Chin. J. Energy Mater.* 2004, 12, 1−12.

(11) Ma, C.; Liu, Z.; Yao, Q. Efficient synthesis of 4-amino-2, 6-dichloropyridine and its derivatives. *Heterocycl. Commun.* 2016, 22, 251−254.

(12) Hollins, R. A.; Merwin, L. H.; Nissan, R. A.; Wilson, W. S.; Gilardi, R. Aminonitropyridines and their N-oxides. *J. Heterocycl. Chem.* 1996, 33, 895−904.

(13) Tang, Y.; He, C.; Imler, G. H.; Parrish, D. A.; Shreeve, J. M. Aminonitro Groups Surrounding a Fused Pyrazolotriazine Ring: A Superior Thermally Stable and Insensitive Energetic Material. *ACS Appl. Energy Mater.* 2019, 2, 2263−2267.

(14) Lee, K.-Y.; Chapman, L. B.; Cobura, M. D. 3-Nitro-1, 2, 4-triazol-5-one, a less sensitive explosive. *J. Energ. Mater.* 1987, 5, 27−33.

(15) Pagoria, P. A comparison of the structure, synthesis, and properties of insensitive energetic compounds. *Propellants, Explos., Pyrotech.* 2016, 41, 452−469.

(16) Terracciano, A.; et al. Degradation of 3-nitro-1, 2, 4-trizole-5-one (NTO) in wastewater with UV/H$_2$O$_2$ oxidation. *Chem. Eng. J.* 2018, 354, 481−491.

(17) Tang, Y.; Huang, W.; Imler, G. H.; Parrish, D. A.; Shreeve, J. M. Enforced planar FOX-7-like molecules: A strategy for thermally stable and insensitive π-conjugated energetic materials. *J. Am. Chem. Soc.* 2020, 142, 7153−7160.

(18) Zhang, J.; Mitchell, L. A.; Parrish, D. A.; Shreeve, J. M. Enforced Layer-by-Layer Stacking of Energetic Salts towards High-Performance Insensitive Energetic Materials. *J. Am. Chem. Soc.* 2015, 137, 10532−10535.

(19) Zhang, J.; Zhang, J.; Parrish, D. A.; Shreeve, J. M. Desensitization of the dinitromethyl group: molecular/crystalline factors that affect the sensitivities of energetic materials. *J. Mater. Chem. A* 2018, 6, 22705−22712.

(20) Yin, P.; Mitchell, L. A.; Parrish, D. A.; Shreeve, J. M. Energetic N-Nitramino/N-Oxyl-Functionalized Pyrazoles with Versatile π−π Stacking: Structure−Property Relationships of High-Performance Energetic Materials. *Angew. Chem., Int. Ed.* 2016, 55, 14409−14411.

(21) Feng, Y.; Deng, M.; Song, S.; Chen, S.; Zhang, Q.; Shreeve, J. M. Construction of an unusual two-dimensional layered structure for fused-ring energetic materials with high energy and good stability. *Engineering* 2020, 6, 1006−1012.

(22) Zhang, W.; Zhang, J.; Deng, M.; Qi, X.; Nie, F.; Zhang, Q. A promising high-energy-density material. *Nat. Commun.* 2017, 8, 181.

(23) Tang, Y.; Kumar, D.; Shreeve, J. M. Balancing Excellent Performance and High Thermal Stability in a Dinitropyrazole Fused 1,2,3,4-Tetrazine. *J. Am. Chem. Soc.* 2017, 139, 13684−13687.

(24) Piercey, D. G.; Chavez, D. E.; Scott, B. L.; Imler, G. H.; Parrish, D. A. An Energetic Triazolo-1, 2, 4-Triazine and its N-Oxide. *Angew. Chem., Int. Ed.* 2016, 55, 15315−15318.

(25) Ye, C.; Gao, H.; Twamley, B.; Shreeve, J. M. Dense energetic salts of N, N′-dinitrourea (DNU). *New J. Chem.* 2008, 32, 317−322.

(26) Huang, Y.; Gao, H.; Twamley, B.; Shreeve, J. M. Highly Dense Nitranilates-Containing Nitrogen-Rich Cations. *Chem. - Eur. J.* 2009, 15, 917−923.

(27) Zhang, P.; et al. Polymorphism, phase transformation and energetic properties of 3-nitro-1, 2, 4-triazole. *RSC Adv.* 2018, 8, 24627−24632.

(28) Li, Y.; Hu, J.; Chang, P.; Wang, B.; Chen, T.; Zhang, H.; Li, P. The synthesis and characteriaztion of 3-dinitromethyl-1,2,4-triazole. *J. Chem. Eng. Chin. Univ* 2019, 33, 141−145.

(29) Lee, J.-S.; Hsu, C.-K.; Chang, C.-L. A study on the thermal decomposition behaviors of PETN, RDX, HNS and HMX. *Thermochim. Acta* 2002, 392, 173−176.

(30) Lee, K.-y.; Giloxdi, R. NTO polymorphs. *MRS Online Proceedings Library (OPL)* 1992, 296, 296.

(31) Zhang, J.; Zhang, Q.; Vo, T. T.; Parrish, D. A.; Shreeve, J. M. Energetic salts with π-stacking and hydrogen-bonding interactions lead the way to future energetic materials. *J. Am. Chem. Soc.* 2015, 137, 1697−1704.

(32) Sayer, J.; Conlon, P. The timing of the proton-transfer process in carbonyl additions and related reactions. General-acid-catalyzed hydrolysis of imines and N-acylimines of benzophenone. *J. Am. Chem. Soc.* 1980, 102, 3592−3600.

(33) Kim, S.; Joe, G. H.; Do, J. Y. Highly efficient intramolecular addition of aminyl radicals to carbonyl groups: a new ring expansion reaction leading to lactams. *J. Am. Chem. Soc.* 1993, 115, 3328−3329.

(34) Wang, Y.; Song, S.; Huang, C.; Qi, X.; Wang, K.; Liu, Y.; Zhang, Q. Hunting for advanced high-energy-density materials with well-balanced energy and safety through an energetic host−guest inclusion strategy. *J. Mater. Chem. A* 2019, 7, 19248−19257.

(35) Hervé, G.; Roussel, C.; Graindorge, H. Selective Preparation of 3, 4, 5-Trinitro-1H-Pyrazole: A Stable All-Carbon-Nitrated Arene. *Angew. Chem., Int. Ed.* 2010, 49, 3177−3181.

(36) Zhang, J.; Hooper, J. P.; Zhang, J.; Shreeve, J. M. Well-balanced energetic cocrystals of H$_5$IO$_6$/HIO$_3$ achieved by a small acid-base gap. *Chem. Eng. J.* 2021, 405, 126623.

(37) Wu, X.; Jin, S.; Zhang, Z.; Jiang, L.; Mu, L.; Hu, Y. S.; Li, H.; Chen, X.; Armand, M.; Chen, L.; Huang, X. Unraveling the storage mechanism in organic carbonyl electrodes for sodium-ion batteries. *Sci. Adv.* 2015, 1, e1500330.

(38) Duan, J.; Yang, S.; Liu, H.; Gong, J.; Huang, H.; Zhao, X.; Zhang, R.; Du, Y. Single crystal SnO$_2$ zigzag nanobelts. *J. Am. Chem. Soc.* 2005, 127, 6180−6181.

(39) Katritzky, A. R.; Murugan, R.; Siskin, M.; Balasubramanian, M. Aqueous high-temperature chemistry of carbo-and heterocycles. 11. Aquathermolysis of arylamines in the presence and absence of sodium bisulfite. *Energy Fuels* 1990, 4, 547−555.

(40) Sahoo, S. K. Renewable and sustainable energy reviews solar photovoltaic energy progress in India: A review. *Renewable Sustainable Energy Rev.* 2016, 59, 927−939.

(41) Singh, A.; Kaur, G.; Sarkar, C.; Mukherjee, N. Investigations on chemical, thermal decomposition behavior, kinetics, reaction mechanism and thermodynamic properties of aged TATB. *Cent. Eur. J. Energ. Mater.* 2018, 15 (2), 258−282.

(42) Tappan, B. C.; Bowden, P. R.; Lichthardt, J. P.; Schmitt, M. M.; Hill, L. G. Evaluation of the detonation performance of insensitive explosive formulations based on 3, 3′ diamino-4, 4′-azoxyfurazan

(DAAF) and 3-nitro-1, 2, 4-triazol-5-one (NTO). *J. Energ. Mater.* **2018**, *36*, 169−178.

(43) Pourmortazavi, S. M.; Rahimi-Nasrabadi, M.; Kohsari, I.; Hajimirsadeghi, S. S. Non-isothermal kinetic studies on thermal decomposition of energetic materials: KNF and NTO. *J. Therm. Anal. Calorim.* **2012**, *110* (2), 857−863.

(44) Wang, K.; Wang, J.; Guo, T.; Wang, W.; Liu, D. Research on the thermal decomposition kinetics and the isothermal stability of HMX. *J. Therm. Anal. Calorim.* **2019**, *135* (4), 2513−2518.

(45) Li, J. S.; Chen, J. J.; Hwang, C. C.; Lu, K. T.; Yeh, T. F. Study on Thermal Characteristics of TNT Based Melt-Cast Explosives. *Propellants, Explos., Pyrotech.* **2019**, *44* (10), 1270−1281.

(46) Pan, Y.; Li, J.; Cheng, B.; Zhu, W.; Xiao, H. Computational studies on the heats of formation, energetic properties, and thermal stability of energetic nitrogen-rich furazano [3, 4-b] pyrazine-based derivatives. *Comput. Theor. Chem.* **2012**, *992*, 110−119.

(47) He, C.; Yin, P.; Mitchell, L. A.; Parrish, D. A.; Shreeve, J. M. Energetic aminated-azole assemblies from intramolecular and intermolecular N−H··· O and N−H··· N hydrogen bonds. *Chem. Commun.* **2016**, *52*, 8123−8126.

(48) Kuhn, B.; Mohr, P.; Stahl, M. Intramolecular hydrogen bonding in medicinal chemistry. *J. Med. Chem.* **2010**, *53*, 2601−2611.

(49) Xiao, H.-M.; Fan, J.-F.; Gu, Z.-M.; Dong, H.-S. Theoretical study on pyrolysis and sensitivity of energetic compounds:(3) Nitro derivatives of aminobenzenes. *Chem. Phys.* **1998**, *226*, 15−24.

(50) Mayer, I. Charge, bond order and valence in the AB initio SCF theory. *Chem. Phys. Lett.* **1983**, *97*, 270−274.

(51) Murray, J. S.; Politzer, P. The electrostatic potential: an overview. Wiley Interdisciplinary Reviews: *Wiley Interdiscip. Rev.: Comput. Mol. Sci.* **2011**, *1*, 153−163.

(52) Murray, J. S.; Concha, M. C.; Politzer, P. Links between surface electrostatic potentials of energetic molecules, impact sensitivities and C−NO$_2$/N−NO$_2$ bond dissociation energies. *Mol. Phys.* **2009**, *107*, 89−97.

(53) Johnson, E. R.; Keinan, S.; Mori-Sánchez, P.; Contreras-García, J.; Cohen, A. J.; Yang, W. Revealing noncovalent interactions. *J. Am. Chem. Soc.* **2010**, *132*, 6498−6506.

(54) Zhang, C.; Cao, X.; Xiang, B. Sandwich complex of TATB/graphene: an approach to molecular monolayers of explosives. *J. Phys. Chem. C* **2010**, *114*, 22684−22687.

(55) Loftsson, T.; Hreinsdôttir, D. Determination of aqueous solubility by heating and equilibration: a technical note. *AAPS PharmSciTech* **2006**, *7* (1), E29−E32.

(56) Del Pilar, A. J. R.; Moises, D. K. S.; Tuscano, R. S. Real Time Rainwater Harvesting System with Built-in Filtration Chamber for Households. Bachelor Thesis. Notre Dame of Marbel University: City of Koronadal, South Cotabato, 2018; pp 10−16.

(57) Reijenga, J.; Van Hoof, A.; Van Loon, A.; Teunissen, B. Development of methods for the determination of pKa values. *Anal. Chem. Insights* **2013**, *8*, S12304.

(58) Fischer, N.; Fischer, D.; Klapötke, T. M.; Piercey, D. G.; Stierstorfer, J. Pushing the limits of energetic materials − the synthesis and characterization of dihydroxylammonium 5,5′-bistetrazole-1,1′-diolate. *J. Mater. Chem.* **2012**, *22*, 20418−20422.

(59) Starchenkov, I.; Andrianov, V.; Mishnev, A. Chemistry of furazano [3, 4-b] pyrazine. 1. Synthesis and thermodynamic appraisal of 4, 8-dihydrodifurazano [3, 4-b, e] pyrazine and its derivatives. *Chem. Heterocycl. Compd.* **1997**, *33*, 216−228.

(60) The room-temperature value was calculated by the volume expansion equation $\rho 298K = \rho T/(1 + \alpha v(298 − T))$; $\alpha v = 1.5 \times 10^{-4}$ K^{-1}.

(61) Suceska, M. *EXPLO5*, version 6.01; Brodarski Institute: Zagreb, Croatia, 2013.

(62) Westwell, M. S.; Searle, M. S.; Wales, D. J.; Williams, D. H. Empirical correlations between thermodynamic properties and intermolecular forces. *J. Am. Chem. Soc.* **1995**, *117*, 5013−5015.

(63) Jenkins, H. D. B.; Tudela, D.; Glasser, L. Lattice potential energy estimation for complex ionic salts from density measurements. *Inorg. Chem.* **2002**, *41*, 2364−2367.

(64) Gao, H.; Ye, C.; Piekarski, C. M.; Shreeve, J. M. Computational characterization of energetic salts. *J. Phys. Chem. C* **2007**, *111*, 10718−10731.

(65) Boultif, A.; Louër, D. Indexing of powder diffraction patterns for low-symmetry lattices by the successive dichotomy method. *J. Appl. Crystallogr.* **1991**, *24* (6), 987−993.